Construction and Building Materials 320 (2022) 126228

Contents lists available at ScienceDirect

Construction and Building Materials

journal homepage: www.elsevier.com/locate/conbuildmat

Modeling of hydration products and strength development for high-volume fly ash binders

Siventhirarajah Krishnya [a], Charith Herath [b], Yogarajah Elakneswaran [a], Chamila Gunasekara [b,*], David W. Law [b], Sujeeva Setunge [b]

[a] Division of Sustainable Resources Engineering, Faculty of Engineering, Hokkaido University, Kita 13, Nishi 8, Kita-ku, Sapporo 060-8628, Japan
[b] Civil and Infrastructure Engineering, School of Engineering, RMIT University, Melbourne, Victoria 3000, Australia

ARTICLE INFO

Keywords:
High-volume fly ash cement paste
Compressive strength
Hydration products
C-S-H
Capillary porosity
Hierarchical model

ABSTRACT

Partial replacement of cement using fly ash, as an environmentally friendly approach, has gained increased attention in construction practice. The realistic prediction of microstructure and mechanical properties of fly ash blended cement paste is therefore noteworthy for many practical applications including selection of construction material and their appraisal of design. In this research work, an integrated framework is proposed and demonstrated for predicting the hydration products and compressive strength of high-volume fly ash binders. The prediction framework is designed to have multiple stages. For computing the hydrates of blended cement paste, a coupled hydration model with thermodynamic modelling is developed. A hierarchical model that captures the development of the paste via multiple levels (from C-S-H globules to blended cement paste) is used subsequently to predict the compressive strength as a function of hydration period. Here, unlike previous works, the formation of C–S–H is realistically modelled by distinguishing it into low- and high-density C–S–H. A series of experiments (including XRD Rietveld analysis, thermo gravimetric analysis, selective dissolution, mercury intrusion porosimetry and compression tests) are performed; hence the predictability of the developed work is assessed by comparing the predicted results with experimental data. A very good agreement is seen between the predicted results (hydration products, pore volume and compressive strength) and experimental results, indicating that the proposed model can be applicable to the high-volume fly ash cement paste to reliably capture the hydrates and compressive strength. It is further noted that with an increase in fly ash replacement ratio, the capillary porosity increases, while the reaction rate and compressive strength decrease.

1. Introduction

Emission of CO_2 (a major greenhouse gas) in the atmosphere is the most serious environmental threat today [1]. It is well known that the production of ordinary Portland cement (OPC) always has been the major source of anthropogenic carbon dioxide, contributing over 6% of the global emission [2]. In particular, nearly 1-ton CO_2 is emitted during the production of 1 ton of OPC [3,4]. Recent studies have demonstrated that the partial replacement of cement using supplementary cementitious materials (SCMs) is one of the most promising alternatives to control the production of OPC, thus minimizing the emission of CO_2 [5,6]. Among the various SCMs, fly ash is one of the most abundantly available industrial waste materials [6], with about 900 million tons of fly ash reported to be generated every year [7]. As per the literature, China produces the highest amount of fly ash, which is around 580 Mt/year [8], followed by India producing around 169.25 Mt/year [9]. The production in USA is around 43.5 Mt/year [10], while it is approximately 14 Mt/year in Australia [11]. One thing is manifest that the approach to utilize the fly ash material in OPC would not only minimize the global production of OPC, but also diminish the issues associated with the disposal of these massive quantities of fly ash [12].

Within the past decade, cement replacement using fly ash has been studied extensively in order to develop binders with similar or improved properties compared to OPC. This has led to the development of high-volume fly ash (HVFA) binders, wherein cement replacement levels vary in a range between 50 and 80%. The fly ash is a well-known pozzolana material, revealing incompetency in reacting with H_2O in the absence of alkaline activator [13]. When the cement replacement level is high, HVFA systems display decreased mechanical properties at early age [14]. The system, however, can achieve comparable later age

* Corresponding author.
E-mail address: chamila.gunasekara@rmit.edu.au (C. Gunasekara).

https://doi.org/10.1016/j.conbuildmat.2021.126228
Received 18 August 2021; Received in revised form 17 November 2021; Accepted 23 December 2021
Available online 30 December 2021
0950-0618/© 2021 Elsevier Ltd. All rights reserved.

strengths due to the slower pozzolanic reaction of fly ash compared to the cement hydration (i.e. due to the absence of required quantities of portlandite ($Ca(OH)_2$) to react with fly ash particles) [13,15–17]. It is worth noting that the loss of early age strength can possibly be compensated by incorporating other additives (such as silica fume, hydrated lime, slag and nano materials including silica and calcium carbonate) to the HVFA system along with the fly ash [4,18–21].

Enhancing the reactivity of fly ash by chemical activation, mechanical activation and thermal treatment were also studied to utilize high amount of fly ash with cement [22–27]. Mixing of concentrated alkali solution such as NaOH, $CaCl_2$, and Na_2SO_4 were found to enhance the pH of the pore solution, accelerating the dissolution of glass phases in the fly ash during the chemical activation [26,27]. The mechanical activation which enhances the reactivity of fly ash by grinding without changing any mineral composition, was proved as one of the efficient ways to improve the reactivity [22–25]. During the grinding process, the particle size of the fly ash decreases, thus improving the reaction rate due to increased specific surface area. During the dry grinding process, however, there is a possibility for agglomeration of grinded particles as the result of high specific energy. At the same time, high efficiency and low energy consumption were reported for wet grinding technology [23,24]. In another case, the mechanical and durability characteristics of combined method that consisted of steam curing and wet grinded fly ash, were investigated by Yang, Zeng, *et al.*,[23] and Yang, Hu, *et al.*, [24]. The outcomes showed that a greater improvement in compressive strength, sulfate attack and carbonation depth were achieved compared to those cured in room temperature without grinding.

As the different types of material combinations result in different mechanical and durability properties, it is crucial to understand the hydration reaction mechanisms in the HVFA systems to verify and clarify the individual experimental data obtained. Analysis techniques including X-ray diffraction (XRD) and thermo gravimetric analysis (TGA) are used to identify hydration products and cementitious phases. The identification of these is critical to the development of new HVFA binders to enable selection of suitable additives, determine their material proportions and to have an understanding regarding the expected properties of the binder.

Blended cement pastes typically consist of calcium silicate hydrate (C-(A)-S-H) and portlandite, and depending on the composition of binder, a considerable amount of ettringite, hydrotalcite, and AFm phases are formed. Though the fly ash is found to undergo pozzolanic reactions, the reaction products and their compositions are not clearly unified. For instance, the formation of C-A-S-H was assumed in Bentz et al. [28], while formation of C-S-H with aluminate hydrates were assumed in Papadakis studies [29]. Thus, in this research work, C-S-H with AFm phases are considered as hydration products of fly ash blended cement. Fly ash is rich in silicate, thus its addition results in reduced Ca/Si ratio in the C-S-H matrix [30,31]. It has been elucidated that the prime hydration product of cement fly ash matrix, C–S–H, tends to form in two distinct morphologies: (i) low density (LD) C–S–H at the surface of cement and fly ash particles and (ii) high density (HD) C–S–H deeper into the particles [13,32]. It is especially important as the hydration of blended cement containing fly ash is more intricate than that of OPC, because of the occurrence of two inter-related and time-reliant processes (i.e., cement hydration and pozzolanic reaction of fly ash) [33,34]. Additionally, (i) the properties of coal that was burned and (ii) the processing techniques (i.e., handling and storage) are used for a large extent in determining the chemical properties of fly ash, which largely differ from that of OPC that has certain intrinsic chemical properties [12]. Therefore, the determination of microstructure and hydration products of fly ash blended cement is essential.

For the purpose of evaluating the hydration products and mechanical properties, several models were proposed in the past for blended cement. HYMOSTRUC [35] is a popular model proposed to predict the development of hydration and microstructure of OPC as a function of chemical composition of cement, w/c, particle size distribution and temperature. Bentz and co-researchers developed a three-dimensional cement hydration model called CEMHYD3D [36]. Unlike the HYMOSTRUC model, the applicability of the CEMHYD3D model covers diverse cementitious materials such as OPC, limestone filler, silica fume, blast furnace slag and fly ash. However, the prediction of early age properties of slag and fly ash are quite limited in CEMHYD3D, because the induction period of SCMs is not realistically considered [28]. In due course, DUCOM model [37] was proposed to predict both the early age properties and durability of cementitious materials (including OPC, slag, fly ash, silica fume and effect of limestone filler). Although the DUCOM model could to a certain degree capture the behavior, detailed chemical interaction with the mineral composition of SCM was not incorporated in the model [37]. There are also few other models such as kinetic hydration model proposed by Schutter [38] and reaction model by Papadakis and co-researchers [29,39] proposed for blended cement.

One thing is apparent that despite the achievements in modelling frameworks with reliable prediction mechanism are still very limited for blended cement. Most of the existing models neglect the volume of C–S–H in predicting the mechanical properties, but instead, they consider either pore space or the proportion of gel to space in cement matrix [36,40]. At the same time, a few models consider only the C-S-H and portlandite as the hydration products of blended cement, while the other hydrates are neglected [37]. In several models, for simplification of the computations, the C–S–H is assumed to be a single matrix with constant gel porosity (which essentially leads to the discounting of the formation of two types of C-S-H) [33,36,41]. It should be noted that to simulate the properties more realistically and to enable a broad application range, the model (i) should integrate all the possible products of hydration and (ii) should eliminate the assumptions described above.

Keeping the limitations of existing works in mind, this research work aims to propose a modelling framework to evaluate the hydration mechanism and compressive strength of HVFA binders. For predicting the hydrates, the coupled hydration-thermodynamic model that has been proposed in our previous work for OPC [42], is extended for high-volume fly ash cement paste. A hierarchical model (capturing the development of blended cement paste from C–S–H globule via three levels) is systematically developed, hence used to predict the compressive strength of the paste in accordance with the detailed microstructure. In this model, the development of two kinds of C–S–H with the independent properties is originally considered. For the evaluation, two types of HVFA are incorporated; one with 65% cement replaced using fly ash and hydrated lime (HVFA-65), and the other one with 80% cement replaced with fly ash and additives (HVFA-80). The simulated results are finally compared with actual experiment results such as compressive strength and XRD Rietveld analysis results to verify the model and to evaluate the hydration mechanism of HVFA systems. All the modelling approaches and the results obtained are discussed comprehensively in subsequent sections.

2. Materials and methods

2.1. Experiment

2.1.1. Materials and testing

The proportions of the two HVFA binder mixes used in this study are presented in Table 1. The cement type used was ASTM-type III (high

Table 1
Mix proportions of binders.

Sample	Paste mix	Cement (kg)	Fly ash (kg)	Lime (kg)	Water (kg)
HVFA-65	35% PC + 57% FA + 8% HL	3.344	5.446	0.764	2.866
HVFA-80	20% PC + 67% FA + 13% HL	1.911	6.401	1.242	2.866

early strength cement) from a commercial supplier, while ASTM class-F (low calcium fly ash), in compliance with AS 3582.1 [43], was obtained from Eraring power station, Australia. The hydrated lime (HL), in compliance with AS 1672.1 [44], was also obtained from a commercial supplier. The chemical compositions of the OPC and fly ash obtained by X-ray fluorescence analysis are shown in Table 2, and the Mineralogical phase composition obtained from quantitative X-ray diffraction (XRD) is shown in Table 3.

Mixes were prepared at the water to binder (w/b) ratio of 0.3, 50×50×50 mm cubic samples were cast for compression tests and selective dissolution experiments. For the compression tests, three number of cubes were tested at 3, 7, 21, 28 and 56 days. For the selective dissolution experiments, the hydration reaction of paste samples was stopped by mixing with acetone and vacuum filtering at desired time intervals. The powder samples (dried) were sieved through a 63-μm sieve, and then stored in sealed bags for the dissolution experiments, X-ray diffraction (XRD) and thermo gravimetric analysis (TGA). The compression test was carried out using a loading rate of 20 MPa/min in accordance with AS 1012.9 [45] using an MTS testing machine. Bruker AXS D4 Endeavour system with a Cu-Kα radiation operated at 40 kV and 35 mA was used for XRD analysis. The TGA analysis was performed using a PerkinElmer STA 6000 thermal analyzer in a N_2 environment with a flow rate of 19.8 mL/min where the samples were heated from 35 °C to 850 °C at the rate of 10 °C/min. Moreover, mercury intrusion porosimetry (MIP) analysis was undertaken using Shimadzu Auto Pore IV 9500 (with the pressure range of 0.5–60000 psia). Prior to that, the specimen was cut into a piece of about 3 mm cube, immersed in acetone for 24 h, and then vacuum dried for 24 h.

2.1.2. Reaction degree of fly ash

The reaction degree of fly ash was obtained using selective dissolution experiments according to the method suggested by Haha. et al [46]. An EDTA/DEA solution was used to dissolve the hydration products and leave the unreacted components within the solution. Initially, a mixture of 250 mL of triethanolamine and 500 mL of water was prepared. This was followed by dissolving 93 g of disodium ethylenediaminetetraacetic acid (EDTA·$2H_2O$) in the same solution. The solution was then transferred into a volumetric flask, and a measured amount of 173 mL diethylamine was added to the solution. Finally, water was filled to make the solution to the final volume equivalent to 1000 mL. For dissolution of each sample, 50 mL of the solution was diluted up to 800 mL with water. The next step was to weigh approximately 1 g of sample powder to the nearest 0.0001 g and sprinkle it on to the surface of the solution. Afterwards, the solution was stirred using a magnetic stirrer at a constant temperature (25 °C) for 30 mins to achieve an effective dissolution of the sample compounds.

A 90 mm diameter Whatman GF/C filter that had been washed using distilled water and dried at 105 °C and weighted to the nearest 0.0001 g, was used to filter the dissolved solution under a suction vacuum. It should be noted that the residue on filter paper was washed at least 5 times using distilled water. The residue + filter paper was then dried at 105 °C for 1 h, followed by the combined weigh measurement to the nearest 0.0001 g.

Table 2
Chemical composition of binders.

Sample	Composition % by weight	
	Fly Ash	Cement
Na_2O	0.46	–
MgO	0.30	1.24
Al_2O_3	16.95	4.41
SiO_2	75.77	17.99
P_2O_5	0.36	0.74
SO_3	0.11	2.35
K_2O	1.54	0.68
CaO	0.92	68.77
TiO_2	0.78	0.29
Fe_2O_3	2.58	3.25

Table 3
Mineralogical phase composition.

Phase composition (wt.%)			
Fly ash		Cement	
Quartz	25.72	C_3S	62.1
Mullite	13.01	C_2S	6.2
Amorphous	61.27	C_3A	7.7
		C_4AF	7.2
		Calcite	7.5
		Gypsum	5.0

In order to calculate the degree of reaction of fly ash as a function of time, the following equations (suggested previously by Haha M. et al [46]) were adopted.

$$\%FA\ reacted = \left(\frac{R_{UP} - R_{HP}}{R_{UP}}\right) \times 100 \quad (1)$$

$$R_{UP} = (R_{OPC} \times \%OPC) + (R_{FA} \times \%FA) + (R_L \times \%L) \quad (2)$$

With, %OPC + %FA +%L = 100%

where, R_{OPC}, R_{FA}, R_L are the residue weights (unreacted component) after the dissolution of OPC, fly ash and lime respectively, while the % OPC, %FA and %L are the %weights of each material in the mixture design. R_{UP} is the calculated residue of the unhydrated blended paste which is the sum of the residues of the unreacted components (R_{OPC}, R_{FA}, R_L) and R_{HP} is the residue of the hydrated blended paste. The calculated reaction degree of fly ash residue weights (RHP) for both HVFA binder samples at different time intervals are presented in Fig. 1.

2.1.3. Quantitative Rietveld analysis

Using a Rigaku MultiFlex X-ray generator with CuKα radiation, the XRD analysis was performed to fine powdered samples mixed with 10 % (by weight) of corundum (α-Al_2O_3). The test was conducted under a tube voltage and current of 40 kV and 40 mA, respectively. The scan speed was maintained at 1° (2θ) per minute, covering the range of 2θ = 5–70° with 0.02° step interval. For quantitative Rietveld analysis, Siroquant (version 4.0, manufacturer: Sietronics) was used. During the analysis, attention was given primarily to the following targets: α- and β-C_2S, monotrinic and triclinic C_3S, cubic C_3A, C_4AF, Portlandite, Ettringite, Gypsum, Bassanite, Monosulfoaluminate and Corundum (α-Al_2O_3). The quantity of C_3S was considered to be the total of measured polymorphic minerals with different crystalline. Using the quantity derived by adding 10% corundum, the amorphous content was determined from the relationship presented in Eq. (3).

$$P = \frac{100}{100 - A}\left(1 - \frac{A}{R}\right)100 \quad (3)$$

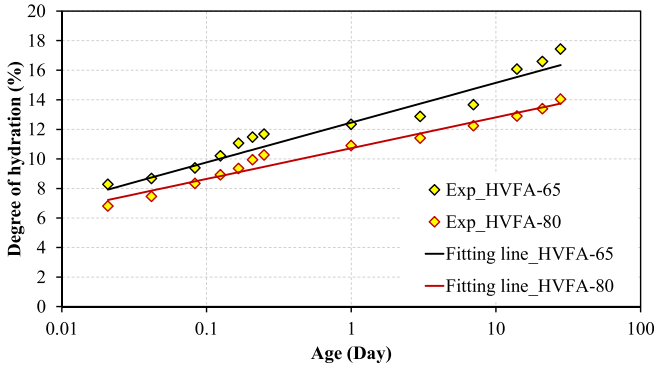

Fig. 1. Degree of hydration of the fly ash in HVFA binders.

where P refers to the quantity of amorphous phase content (as % by mass); A refers to the mixing rate of corundum (as % by mass); R refers to the quantitative value of corundum (as % by mass). The calculated quantity of amorphous in the sample (Rietveld analysis carried out to corundum blended specimen) was used for correcting the determined values of cement minerals. The ignition loss that has been taken from the mass loss occurred as the result of temperature change between 105 °C and 950 °C, was used to correct the value obtained from Rietveld analysis using Eq. (4), hence, to determine the hydration degree against the un-hydrated material.

$$Q = \frac{100}{100 - LOI} Q_0 \tag{4}$$

where, Q refers to the corrected quantity (as %); Q_0 refers to the quantity before the correction (as %); and LOI is the loss of ignition (as %).

2.2. Modelling procedure

Within the past decade, several hydration models have been proposed and applied for OPC system. In order to develop a model for predicting hydration reactions of fly ash blended cement, extension of an existing model (of Portland cement) is considered as an optimal approach, because its predictability has already evaluated along with adequate validations. In this work, the model developed previously by Krishnya *et al.* [42] to compute the microstructure and mechanical characteristics of OPC, is amended to predict the hydration products and compressive strength of high-volume fly ash blended cement. The computation integrates the hydration model, thermodynamic model, prediction of volume fraction and hierarchical model.

The cement hydration model adopted herein was initially proposed by Parrot and Killoh [47]. As substantiated in many previous works [41,48–50], the model could be reliable for predicting the dissolution rate of clinker minerals as a function of hydration time. Additionally, the reaction rate of fly ash for the two HVFA binders were computed with hydration period based on the experimental results depicted in Fig. 1. Studies also showed that the model coupled with set of thermodynamic databases could be applicable for predicting the chemical composition and phase assemblage of hydrate [48,51]. Here, the Geochemical software called IPHREEQC was used to perform the thermodynamic calculations. The IPHREEQC is an open-source package, and that was repeatedly involved in predicting the hydration products of wide range of cementitious materials [52–54]. It should be noted that in this proposed model, the clinker and fly ash were considered as kinetic reaction, and hydrated lime was considered as thermodynamic equilibrium reaction.

In the model proposed by Krishnya *et al.* [42], the development of two kinds of C-S-H (LD and HD C-S-H) was incorporated for jennite type C-S-H. In the case of fly ash binders, the CaO/SiO_2 ratio is lower compared to that of cement paste [55,56]. Therefore, as the preliminary step, the properties of two types of C-S-H in fly ash binders were amended based on the available experiment results. Due to the molar volume difference between hydrates and binders, a reduction can generally be witnessed in the total hydrates compared to reactants at initial stage (i.e., prior to the reactions). This difference, in the field of cement chemistry, is broadly designated as chemical shrinkage. The chemical shrinkage coefficient for fly ash determined from the experimental results was additionally included in the OPC paste model. Based on the volume fractions of two types of C-S-H, other hydration products and chemical shrinkage, the capillary porosity in the fly ash cement matrix was computed and verified with raw experiment data and the data available in literature.

Fig. 2 displays the three consecutive levels of the hierarchical model proposed to predict the compressive strength of binders. The C–S–H globules comprising of both LD and HD C–S–H were considered in Level 1 at the characteristic scale of 1–100 nm. In Level 2, capillary pores were additionally considered with C–S–H globules at the 100 nm–10 μm scaling (designated as C–S–H foam). Finally, the unreacted fly ash, clinker minerals and other hydration products were further accumulated to the system (Level 3) at characteristic scale ranging between 10 and 100 μm. The initial input parameters for the hierarchical model were the volume fraction of each matrix in the hydrated paste. It should be mentioned that the predicted properties from the previous level are the input parameters for the subsequent levels. Further detail and fundamental formulas used in the model can be found in Krishnya *et al.* [42].

3. Results and discussion

3.1. Model validation

3.1.1. Validation of chemical shrinkage

The chemical shrinkage verses hydration period for pure OPC and 35 % of fly ash mixture (w/c of 0.5) is presented in Fig. 3, comparing the predicted results with the experimental data reported by De Weerdt *et al.* [57]. The chemical shrinkage coefficients of clinker minerals (C_3S, C_2S, C_3A and C_4AF) and the validation of chemical shrinkage for pure OPC are detailed in Krishnya et al., [42]. For the reacted fly ash, the chemical shrinkage coefficient is assumed to be 0.2 mL/g of reacted fly ash. The predicted results for fly ash mixture and OPC show a very good agreement with experimental results. For instance, the experiment results of chemical shrinkage after 28 days for fly ash mixture and OPC are 0.071 and 0.056 mL/g of OPC, while the predicted results are 0.068 and 0.056 mL/g of OPC, respectively. As per the prediction, the quantity of chemical shrinkage increases with the hydration period, which precisely captures the tendency observed in the experiment results. A similar

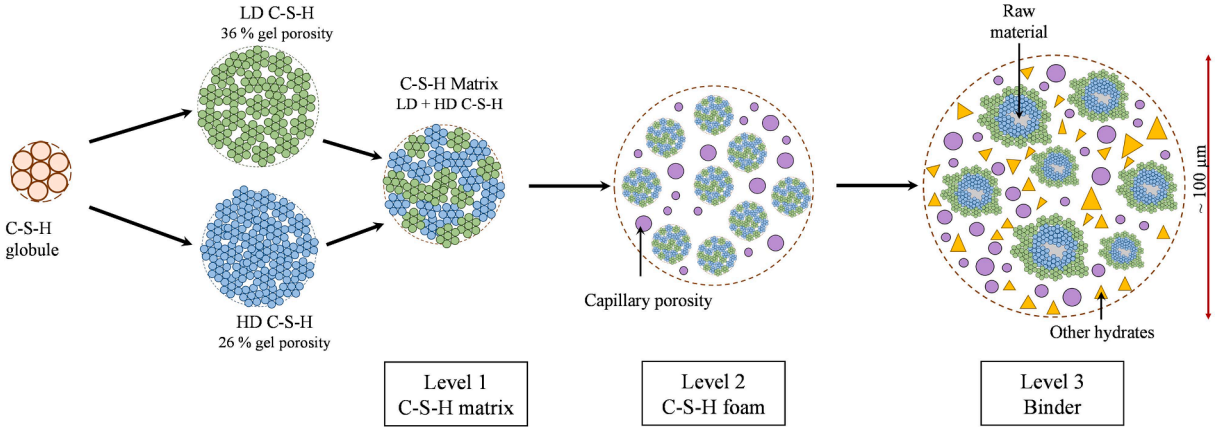

Fig. 2. Three consecutive levels of Hierarchical model: (Level 1) C-S-H globule, (Level 2) C-S-H foam, and (Level 3) binder.

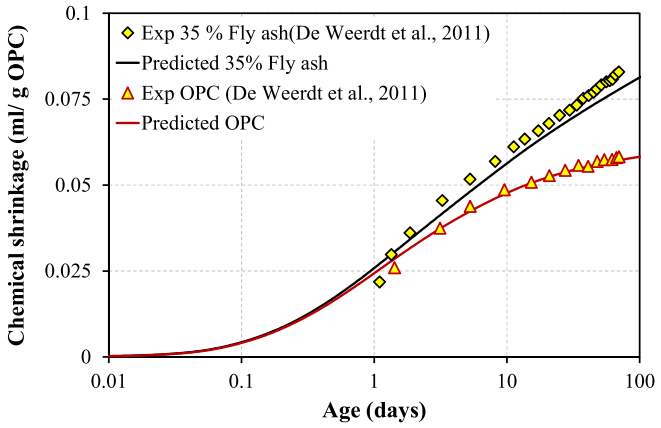

Fig. 3. Variation of chemical shrinkage with hydration period for OPC and fly ash matrix.

tendency has also been reported by several other researchers [30,57,58]. During the hydration period, hydrates increase due to the hydration reaction in cementitious materials, and as the result, the volume reduction increases with hydration reaction due to molar volume effect.

3.1.2. *Validation of porosity in fly ash system*

The variations of porosity and capillary porosity with hydration period are shown in Fig. 4 and Fig. 5, respectively. The capillary porosity of the binder was computed from variance between initial (fly ash, clinker and water) and final volume (unreacted raw materials, hydrates, and chemical shrinkage) of the matrix. It should be noted that the variation of porosity for pure OPC system has been already validated in our previous work [42]. Here, for the volumetric prediction of hydration products and prediction of capillary porosity, the properties of C-S-H in the fly ash matrix required modification. Many previous studies highlighted that the Ca/Si ratio of C-S-H in OPC fly ash binder (~1.5) is lower compared to that of pure OPC system (~1.7) because of the additional silica (Si) supplied from the dissolution process of the fly ash during hydration reaction [29,30,33,55,56]. Furthermore, the density of C-S-H decreases with the decrease in Ca/Si ratio [59,60]. To the best the of authors' knowledge, the densities of LD C-S-H and HD C-S-H for the C-S-H of 1.5 Ca/Si ratio have not been reported thus far; therefore, the properties of the two types C-S-H were modified based on the available experiment results.

The MIP experiment results for porosity of 50 % fly ash mixture with 0.5 w/b ratio obtained from Liu *et al.* [55] are compared in Fig. 4 with predicted results of modified C-S-H properties for fly ash binders (LD C-S-H density 1.4 g/cm^3 and HD C-S-H 1.7 g/cm^3) and existing C-S-H properties for pure OPC system (LD C-S-H density 1.7 g/cm^3 and HD C-S-H 2.0 g/cm^3). The MIP experiment method determines the porosity that is correspondent to the size of pore above 3 nm (in diameter), which literally covers the entire capillary porosity and a part of gel porosity [61]. Thus, MIP results are comparable with the sum total of capillary porosity and gel porosity of LD C-S-H which has the larger pore size compared to HD C-S-H. The predicted results illustrated in Fig. 4 are the summation of capillary porosity and gel porosity of LD C-S-H. As illustrated, the prediction shows a very good agreement when the densities of LD and HD C-S-H are reduced to 1.4 and 1.7 g/cm^3 , respectively. It should be noted that the predicted results of capillary porosity reveal a maximum deviation of 5% compared to the experiment results.

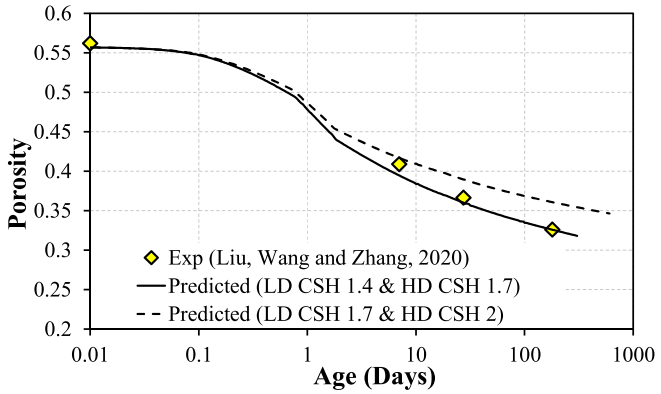

Fig. 4. Verification of porosity with hydration period of OPC fly ash matrix.

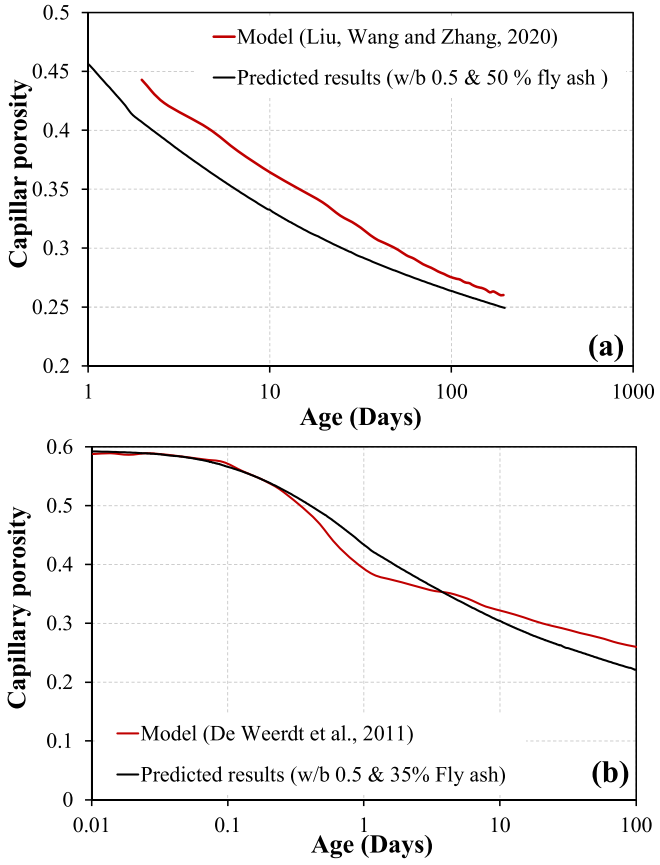

Fig. 5. Validation of capillary porosity with hydration period with previously available model results: (a) modeling results from Liu *et al.* [55] (b) modeling results from De Weerdt *et al.*[57]

In Fig. 5, the predictability of the proposed capillary porosity model for fly ash matrix is compared with previously develop models such as CEMHYD3D [55] and the one proposed by De Weerdt *et al.* [57]. The CEMHYD3D model was developed using the digital image of 3D microstructure to predict the porosity and hydration products [36], while the model developed by De Weerdt *et al.* [57] was based on the thermodynamic calculation using GEMS software package. The maximum variation between the proposed model and existing models is only 8 %, revealing a better predictability for capillary porosity.

3.2. *Hydration and microstructure of HVFA paste and OPC paste*

Following the successful validation of the extended model for fly ash binder, the hydration products and unreacted raw material were predicted using the proposed model. Fig. 6 illustrates the comparison between the predicted results and the experiment results of quantitative values from XRD Rietveld analysis for the HVFA-65 and HVFA-80. The amorphous content indicated in predicted results includes the amorphous component in fly ash, C-S-H, monocarboaluminate, hydrotalcite

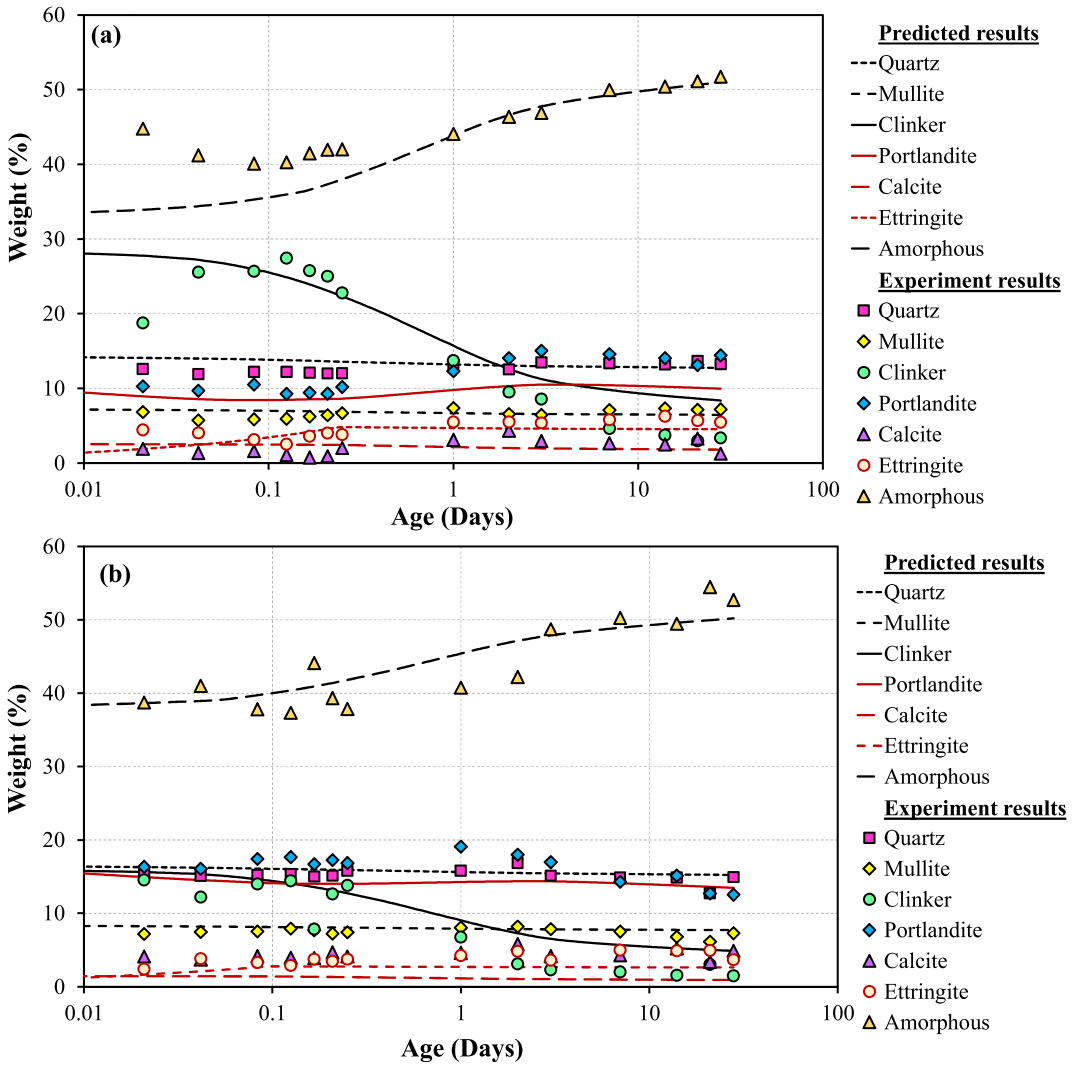

Fig. 6. Quantitative comparison between predicted values and the values determined from XRD Rietveld analysis of HVFA binders for w/b 0.3 (a) HVFA-65 and (b) HVFA-80.

and Fe-siliceous hydrogarnet. It is evident that the computed results of hydrates demonstrate an excellent consistency with experiment data for both binders (HVFA-65 and HVFA-80). Initially, the amorphous content is high in HVFA-80 compared to HVFA-65 due to the high quantity fly ash. With the hydration period, the content increases in both binders, which is principally due to the formation of C-S-H and Fe-siliceous hydrogarnet. On the other hand, the predicted percentage of clinker decrease with the time for both cases, which replicates the tendency of the experiment results to a reasonable degree. This could be attributed to the dissolution of the clinker during the hydration reaction. However, in Fig. 6(a), the experimental results of clinker phases show an increasing tendency up to 0.1 day. It is therefore understandable that the first two experimental points of clinker might be associated with certain error. Moreover, the total amount of amorphous phase has been calculated by simple subtraction (i.e. (100- total crystalline) %.); thereby, the error in clinker phase might also influence the results of amorphous phase up to 0.1 day.

The amount of quartz and mullite remain constant with hydration period, as they do not have any reaction with the water. Moreover, in the early stages, there is a considerable quantity of portlandite in both HVFA binders, which is possibly from the manually added hydrated lime (to improve the pozzolanic reaction of fly ash system) [17,30]. During the hydration reaction, the portlandite is observed to decrease to a certain concentration, followed by subsequent increase. In particular, a notable increase is observed after 1-day hydration for both binders (refer Fig. 6). A possible explanation is that at the early age, the portlandite contributes to the pozzolanic reaction with SiO_2 in fly ash to produce C-S-H. However, as newly formed portlandite is added to the system as the result of the progressive hydration reaction of clinker, this leads to an increase in total amount of portlandite later in the process.

Regarding the capillary porosity of HVFA cement paste, the predicted and experiment results of pore volume of cement pastes with 65 % (HVFA-65) and 80 % (HVFA-80) replacement of fly ash and hydrated lime using MIP are depicted in Fig. 7. The predicted pore volume which is the summation of gel pores of LD C-S-H and capillary pores is based on detail microstructure of hydrates and chemical shrinkage of clinker minerals and fly ash. As depicted in Fig. 7, the predicted pore volume and experiment results reveal a good consistency for the high-volume fly ash cement, indicating that the pore volume decreases with curing age at a decreasing rate. The tendency observed herein corresponds to the development of the hydration products during the hydration, which progressively leads to the decrease in pore volume. Due to the space occupied by water in binder matrix, the pore volume is high in the early stages. However, as hydration progresses, the hydration products formed tend to plug the pore spaces, thus resulting in a hardened matrix with condensed porosity. Correspondingly, the reduction in the porosity is equivalent to the rise in the hydration products. Similar trends in porosity were also reported in several earlier works in cement paste as

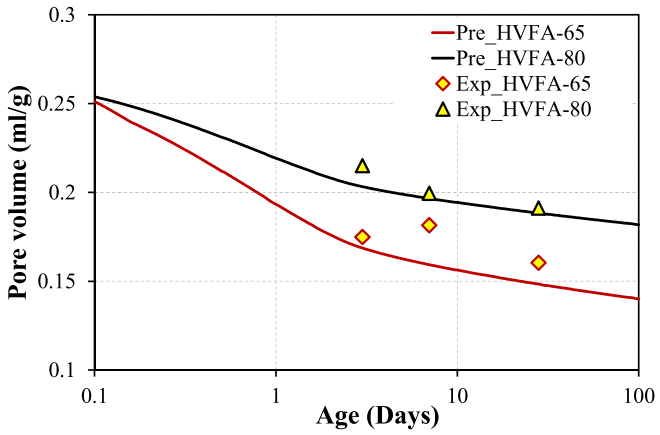

Fig. 7. Validation of predicted pore volume with aging time for w/b of 0.3.

well as in blended cement matrix [42,55,57,61,62]. It should be indicated that there is, however, the experimental results of HVFA-65 show an increasing tendency between 3 and 7 days, which could possibly be attributed to experimental error, thus requiring further corroboration in future work. Furthermore, the pore volume in the cement matrix appears to increase with the replacement ratio of fly ash (Fig. 7). This can be explained by the reaction rate of fly ash (refer to Fig. 1). Many previous studies found that the replacement ratio is one of the important factors determining the hydration rate of fly ash system [55,56]. Owing to lower pH and Ca^{2+} concentration, activated ability of the pore solution is hindered at higher fly ash replacement ratio [40,55]; which, as a result, decreases the formation rate of hydration products, and hence leads to higher porosity in high fly ash mixes.

Fig. 8 illustrates the hydration products computed using thermodynamic calculations. Raw material and capillary porosity are high in the early age of hydration as shown in Fig. 8. With the increase in hydration time, the volume of clinker minerals and fly ash tends to decrease (as hydration takes place), which in turn results in a surge in hydrates. When comparing the hydrates of OPC and the two HVFA binders, the amount of hydration products except monocarboaluminate decreases with increasing replacement content of fly ash due to the low cement content and low degree of reactivity of the fly ash binders. The high content of monocarboaluminate obtained in HVFA binders compared to pure OPC could be possibly due to the additional amount of Al from fly ash and portlandite from hydrated lime [29,39,55]. In this proposed model, Al incorporated with C-S-H is not considered for the prediction of hydrates of fly ash blended cement, which is in consistent with assumption made by Papadakis [29]. The chemical shrinkage due to volume reduction of hydrates is higher in pure cement paste compared to that of HVFA. It is well known that the pure OPC paste has high reaction rate compared to HVFA binders; thus, a high-volume reduction could be obtained with a low fly ash content. Nevertheless, very low capillary porosity is predicted for OPC paste which has a high degree of reaction and low concentration of unreacted minerals.

3.3. Prediction of compressive strength

The variation of compressive strengths (computed and experimental) with hydration period for the type I OPC (supplied by Cement Australia) of w/c 0.4 is depicted in Fig. 9. The experiment results for the pure OPC system were taken from Zhou *et al.* [63]. The validation of the proposed compressive strength model for OPC with the w/c from 0.3 to 0.6 has been previously verified with different experimental data sets [42]. The data (in Fig. 9) demonstrates that the model is applicable to the Australian OPC as well. Following verification, the model was amended to predict the compressive strength of high-volume fly ash binders. The C-S-H and capillary porosity are respectively known to be the prime active bonding phase and weakest zone in the hardened cement matrix. Therefore, the emphasis is essentially given on the two kinds of C-S-H and capillary porosity to predict the compressive strength over the hydration period. Further information and formulas used for the prediction can be found in Krishnya *et al.* [42]. Since the volume of hydration products and capillary porosity are the required input parameters for the model, the weight assemblage of hydrates including amorphous contents (see Fig. 6) and capillary porosity (see Fig. 7) are verified from the experimental results.

Fig. 10 presents the evolution of compressive strength for HVFA matrix of w/b 0.3. The proposed model shows excellent results in predicting the compressive strength for the two HVFA matrix across the hydration period. However, the model slightly underestimates the compressive strength after 28 days hydration for HVFA-80, and a sharp increase is also seen in experimental results after 28 days (Fig. 10), whereas no such variations are witnessed in the reaction rates (refer to Fig. 1). It is well known that the hydration reaction of fly ash is slower that of cement matrix, and its contribution to strength occurs at later age [18,64]. In this proposed model, the relationship between reaction degree of fly ash and hydration period has been derived based on the raw experimental results only up to 28 days. There is a possibility for the reaction degree to show higher incremental rate at later age. This might probably be one major reason for underestimating the strength of HVFA-85 mixture after 28 days. Therefore, to generalize the model, it is necessary to validate with more experimental data corresponding to different replacement ratio of fly ash for HVFA binders.

The predicted compressive strength results (Fig. 10) show an increasing tendency with hydration period for both pure OPC system as well as HVFA binders. This could be attributable to two major factors: (i) the increase in hydration products (mainly C-S-H) (see Fig. 8) and (ii) the decrease in capillary porosity (see Fig. 7) with time [63,65,66]. Moreover, the compressive strength decreases with increasing replacement of fly ash. Similar findings were also observed by other research works [66–68]. This could possibly be related to the reaction rate of fly ash (Fig. 1) and the capillary porosity (Fig. 7). As pointed out in the previous section, the reaction rate of fly ash decreases with the increase in fly ash content. The increase in fly ash content leads the microstructure to contain more capillary pores, which eventuates in lower compressive strength.

To reliably predict the compressive strengh of HVFA binders, the C-S-H distribution factor (β) was incorporated in the proposed model. Generally, the amorphous C–S–H gel resides in the prime hydration product in the hardened paste; therefore, the gradient of its distribution greatly determines the mechanical properties. β, the factor defining the spatial distribution (i.e., the gradient) of C–S–H within the matrix, would typically be in a range between 0.4 and 1.0, depending on numerous properties including cement fineness, heterogeneous nucleation, w/c and precipitation of C–S–H [69]. It should be mentioned that the 0.9 of β value corresponded to the best fit for HVFA-65, while this was 1.0 for HVFA-80. The prediction elucidates an increasing tendency of β with fly ash replacement ratio, which displays a good agreement with the similar observed tendency for w/c ratio [42]. One possible reason may be that a high quantity of fly ash which provides high number of unreacted particles, helps to evenly distribute the C-S-H precipitated compared to a low fly ash content. The observed trend of β, however, has not been fully evaluated, as yet, to cover all replacement ratios of fly ash. Therefore, an extensive study on β is herein recommended for the future work.

4. Conclusions

In this study, an integrated modelling framework was proposed to predict the microstructure and compressive strength of high-volume fly ash cement paste. A cement hydration model was reliably coupled with thermodynamic calculations and the reaction degree of fly ash to simulate the hydration products. The compressive strength of binder

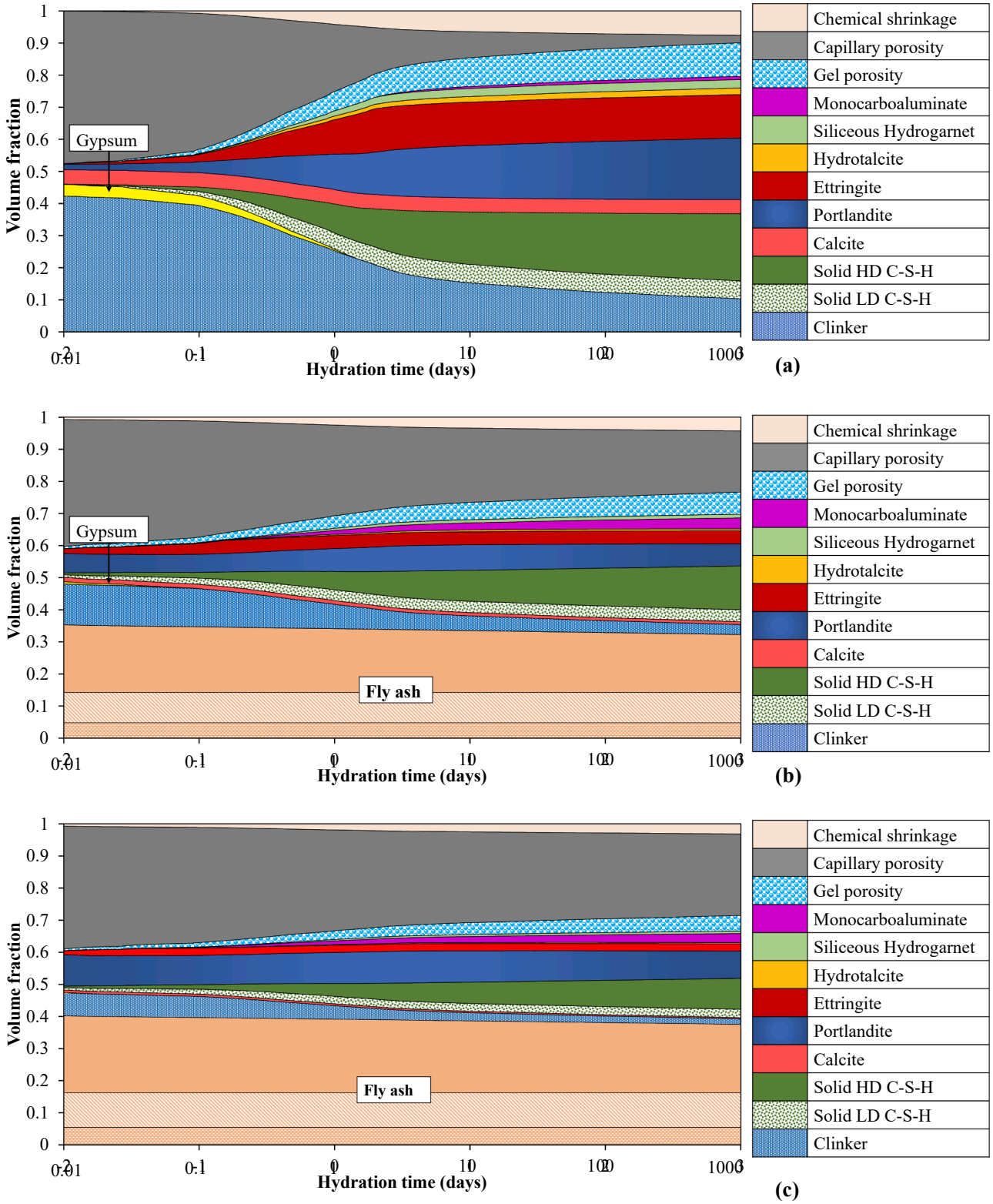

Fig. 8. Volume fraction of hydration products as the function of hydration time for w/b 0.3 (a) OPC, (b) HVFA-65 and (c) HVFA-80.

was predicted using a hierarchical model initiating from C-S-H and concluding with binder matrix. The predicted results of the hydration products and compressive strength were compared with experimental results to check the predictability of the proposed model. A number of experimental techniques were performed to evaluate the reaction degree and microstructure of the binders utilizing different replacement ratios of fly ash (HVFA-65 and HVFA-80). To correlate the microstructure with mechanical properties, compressive strength tests were performed for the two fly ash binders. Based on the outcomes attained from this proposed work, the following conclusions can be drawn:

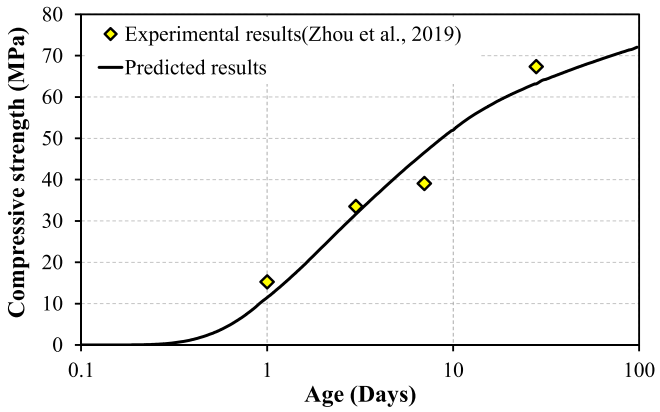

Fig. 9. Validation of compressive strength of the OPC with respect to the aging time for w/c of 0.4.

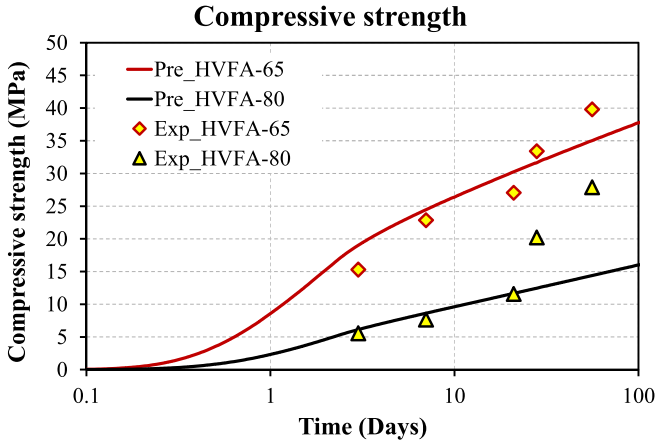

Fig. 10. Evolution of compressive strength of HVFA binders with aging time for w/b 0.3.

1. The predicted hydration products such as amorphous, portlandite, ettringite and unreacted raw materials with curing period provided excellent consistency with the experimental results for fly ash binders with different replacement ratios.
2. By considering the chemical shrinkage of the clinker minerals and the fly ash and two types of C-S-H gel, the capillary porosity of the fly ash binder was computed. The predicted results corresponded very well with the actual values obtained from the MIP data for the two fly ash binders.
3. Simulated compressive strength results over the hydration period were compared with the measured compressive strength values to determine the predictability of the hierarchical model proposed for high-volume fly ash cement paste. The predicted results of HVFA-65 showed a fairly good agreement with experiment results. However, the predictions slightly underestimated the compressive strength of HVFA-80 after 21 days; thereby, further validations are recommended with different replacement ratio for longer age mechanical properties.
4. Both measured and predicted results indicated that the reaction degree, pore structure and compressive strength of high-volume fly ash cement system are highly related with replacement ratio of fly ash and curing age. To enhance the applicability of the model towards the future, it is appropriate to define a C-S-H distribution factor with different replacement ratio of fly ash as well as with different w/b ratios. This is an important point to be addressed in the future work.

Declaration of Competing Interest

The authors declare that they have no known competing financial interests or personal relationships that could have appeared to influence the work reported in this paper.

References

[1] M.E. Bildirici, Cement production, environmental pollution, and economic growth: evidence from China and USA, Clean Technol. Environ, Policy. 21 (2019) 783–793.
[2] J. Xie, J. Wang, R. Rao, C. Wang, C. Fang, Effects of combined usage of GGBS and fly ash on workability and mechanical properties of alkali activated geopolymer concrete with recycled aggregate, Compos. Part B Eng. 164 (2019) 179–190.
[3] G. Kürklü, The effect of high temperature on the design of blast furnace slag and coarse fly ash-based geopolymer mortar, Compos. Part B Eng. 92 (2016) 9–18.
[4] C. Gunasekara, M. Sandanayake, Z. Zhou, D.W. Law, S. Setunge, Effect of nano-silica addition into high volume fly ash–hydrated lime blended concrete, Constr. Build. Mater. 253 (2020), 119205.
[5] S.M. Monteagudo, A. Moragues, J.C. Gálvez, M.J. Casati, E. Reyes, The degree of hydration assessment of blended cement pastes by differential thermal and thermogravimetric analysis. Morphological evolution of the solid phases, Thermochim. Acta. 592 (2014) 37–51.
[6] I. Ignjatović, Z. Sas, J. Dragaš, J. Somlai, T. Kovács, Radiological and material characterization of high volume fly ash concrete, J. Environ. Radioact. 168 (2017) 38–45.
[7] C. Heidrich, H. Feuerborn, A. Weir, Coal Combustion Products : a Global Perspective, (2013).
[8] NDRC, in Annual Report on Comprehensive Utilization of Resources in China (2014). National Development and Reform Commission: China., 2014.
[9] CEA, Report on Fly Ash Generation at Coal/Lignite Based Thermal Power Stations and its Utilization in the Country for the year 2016-17 CENTRAL ELECTRICITY AUTHORITY, 2016.
[10] ACAA, in 2016 Coal Combustion Product (CCP) Production and Use Survey Report. American Coal Ash Association: Farmington Hills., 2016.
[11] ADAA, Ash Development Association of Australia Annual Membership Survey Results, in H. G. P. Ltd, ed. Ash Development Association of Australia., 2016.
[12] M. Ahmaruzzaman, A review on the utilization of fly ash, Prog. Energy Combust. Sci. 36 (2010) 327–363.
[13] Q. Zeng, K. Li, T. Fen-Chong, P. Dangla, Determination of cement hydration and pozzolanic reaction extents for fly-ash cement pastes, Constr. Build. Mater. 27 (2012) 560–569.
[14] C. Herath, C. Gunasekara, D.W. Law, S. Setunge, Performance of high volume fly ash concrete incorporating additives: A systematic literature review, Constr. Build. Mater. 258 (2020), 120606.
[15] C.D. Atiş, High-Volume Fly Ash Concrete with High Strength and Low Drying Shrinkage, J. Mater. Civ. Eng. 15 (2003) 153–156.
[16] C.H. Huang, S.K. Lin, C.S. Chang, H.J. Chen, Mix proportions and mechanical properties of concrete containing very high-volume of Class F fly ash, Constr. Build. Mater. 46 (2013) 71–78.
[17] S.A. Barbhuiya, J.K. Gbagbo, M.I. Russell, P.A.M. Basheer, Properties of fly ash concrete modified with hydrated lime and silica fume, Constr. Build. Mater. 23 (2009) 3233–3239.
[18] A.M. Rashad, Potential Use of Silica Fume Coupled with Slag in HVFA Concrete Exposed to Elevated Temperatures, J. Mater. Civ. Eng. 27 (2015) 04015019.
[19] X.H. Ling, S. Setunge, I. Patnaikuni., Effect of different concentrations of lime water on mechanical properties of high volume fly ash concrete, in: 22nd Australas. Conf. Mech. Struct. Mater. ACMSM 2012. Sydney, NSW, 2013.
[20] R. Roychand, S. De Silva, D. Law, S. Setunge, Micro and Nano Engineered High Volume Ultrafine Fly Ash Cement Composite with and without Additives, Int. J. Concr. Struct. Mater. 10 (2016) 113–124.
[21] F.U.A. Shaikh, S.W.M. Supit, Mechanical and durability properties of high volume fly ash (HVFA) concrete containing calcium carbonate (CaCO3) nanoparticles, Constr. Build. Mater. 70 (2014) 309–321.
[22] J. Yang, J. Huang, Y. Su, X. He, H. Tan, W. Yang, B. Strnadel, Eco-friendly treatment of low-calcium coal fly ash for high pozzolanic reactivity: A step towards waste utilization in sustainable building material, J. Clean. Prod. 238 (2019), 117962.
[23] J. Yang, L. Zeng, X. He, Y. Su, Y. Li, H. Tan, B. Jiang, H. Zhu, S.K. Oh, Improving durability of heat-cured high volume fly ash cement mortar by wet-grinding activation, Constr. Build. Mater. 289 (2021), 123157.
[24] J. Yang, H. Hu, X. He, Y. Su, Y. Wang, H. Tan, H. Pan, Effect of steam curing on compressive strength and microstructure of high volume ultrafine fly ash cement mortar, Constr. Build. Mater. 266 (2021), 120894.
[25] N. Marjanović, M. Komljenović, Z. Baščarević, V. Nikolić, Improving reactivity of fly ash and properties of ensuing geopolymers through mechanical activation, Constr. Build. Mater. 57 (2014) 151–162.
[26] M. Sadique, H. Al-Nageim, W. Atherton, L. Seton, N. Dempster, Mechano-chemical activation of high-Ca fly ash by cement free blending and gypsum aided grinding, Constr. Build. Mater. 43 (2013) 480–489.
[27] I. Wilińska, B. Pacewska, Influence of selected activating methods on hydration processes of mixtures containing high and very high amount of fly ash: A review, J. Therm. Anal. Calorim. 133 (2018) 823–843.
[28] D.P. Bentz, S. Remond, Incorporation of Fly Ash into a 3-D Cement Hydration microstructure Model, National Institute of Standards and Technology, US, 1997.

[29] V.G. Papadakis, Effect of fly ash on Portland cement systems: Part I. Low-calcium fly ash, Cem. Concr. Res. 29 (1999) 1727–1736.
[30] F. Deschner, F. Winnefeld, B. Lothenbach, S. Seufert, P. Schwesig, S. Dittrich, F. Goetz-Neunhoeffer, J. Neubauer, Hydration of Portland cement with high replacement by siliceous fly ash, Cem. Concr. Res. 42 (2012) 1389–1400.
[31] B. Lothenbach, K. Scrivener, R.D. Hooton, Supplementary cementitious materials, Cem. Concr. Res. 41 (2011) 1244–1256.
[32] P.D. Tennis, H.M. Jennings, A model for two types of calcium silicate hydrate in the microstructure of Portland cement pastes, Cem. Concr. Res. 30 (2000) 855–863.
[33] X.Y. Wang, H.S. Lee, Modeling the hydration of concrete incorporating fly ash or slag, Cem. Concr. Res. 40 (2010) 984–996.
[34] F. Moghaddam, V. Sirivivatnanon, K. Vessalas, The effect of fly ash fineness on heat of hydration, microstructure, flow and compressive strength of blended cement pastes, Case Stud. Constr. Mater. 10 (2019), e00218.
[35] G. Ye, X. Liu, A.M. Poppe, G. De Schutter, K. Van Breugel, Numerical simulation of the hydration process and the development of microstructure of self-compacting cement paste containing limestone as filler, Mater. Struct. Constr. 40 (2007) 865–875.
[36] D.P. Bentz, CEMHYD3D: A Three-Dimensional Cement Hydration and Microstructure Development Modeling Package, Autom. Constr. 8 (1999) 227–235.
[37] K. Maekawa, T. Ishida, T. Kishi, Multi- scale modeling of structural concrete, 2009.
[38] G. De Schutter, L. Taerwe, Degree of hydration-based description of mechanical properties of early age concrete, Mater. Struct. Constr. 29 (1996) 335–344.
[39] V.G. Papadakis, Effect of fly ash on Portland cement systems. Part II. High-calcium fly ash, Cem. Concr. Res. 30 (2000) 1647–1654.
[40] L. Lam, Y.L. Wong, C.S. Poon, Degree of hydration and gel/space ratio of high-volume fly ash/cement systems, Cem. Concr. Res. 30 (2000) 747–756.
[41] F. Lavergne, A. Ben Fraj, I. Bayane, J.F. Barthélémy, Estimating the mechanical properties of hydrating blended cementitious materials: An investigation based on micromechanics, Cem. Concr. Res. 104 (2018) 37–60.
[42] S. Krishnya, Y. Yoda, Y. Elakneswaran, A two-stage model for the prediction of mechanical properties of cement paste, Cem. Concr. Compos. 115 (2021), 103853.
[43] AS/NZS 3582.1:2016 Supplementary cementitious materials - Part 1: Fly ash. Standards Australia, (2016).
[44] AS 1672.1, Australian Standard ® Limes and limestones Part 1: Limes for building, 1997.
[45] AS 1012.9:2014 | Method For Testing Concrete Specimens | SAI Global, (2014).
[46] M. Ben Haha, K. De Weerdt, B. Lothenbach, Quantification of the degree of reaction of fly ash, Cem. Concr. Res. 40 (2010) 1620–1629.
[47] L.J. Parrot, D.C. Killoh, Prediction of cement hydration, in: Br. Ceram. Proc., 1984: pp. 35, 41–53.
[48] X. Ke, Y. Duan, Coupling machine learning with thermodynamic modelling to develop a composition-property model for alkali-activated materials, Compos. Part B Eng. 216 (2021), 108801.
[49] B. Lothenbach, T. Matschei, G. Möschner, F.P. Glasser, Thermodynamic modelling of the effect of temperature on the hydration and porosity of Portland cement, Cem. Concr. Res. 38 (2008) 1–18.
[50] Y. Elakneswaran, E. Owaki, S. Miyahara, M. Ogino, T. Maruya, T. Nawa, Hydration study of slag-blended cement based on thermodynamic considerations, Constr. Build. Mater. 124 (2016) 615–625.
[51] B. Lothenbach, D.A. Kulik, T. Matschei, M. Balonis, L. Baquerizo, B. Dilnesa, G. D. Miron, R.J. Myers, Cemdata18: A chemical thermodynamic database for hydrated Portland cements and alkali-activated materials, Cem. Concr. Res. (2019).
[52] T. Zhang, H. Chen, X. Li, Z. Zhu, Hydration behavior of magnesium potassium phosphate cement and stability analysis of its hydration products through thermodynamic modeling, Cem. Concr. Res. 98 (2017) 101–110.
[53] Y. Elakneswaran, N. Noguchi, K. Matumoto, Y. Morinaga, T. Chabayashi, H. Kato, T. Nawa, Characteristics of Ferrite-Rich Portland Cement: Comparison With Ordinary Portland Cement, Front. Mater. 6 (2019) 1–11.
[54] S. Krishnya, Y. Elakneswaran, Y. Yoda, Proposing a three-phase model for predicting the mechanical properties of mortar and concrete, Mater. Today Commun. 29 (2021), 102858.
[55] C. Liu, F. Wang, M. Zhang, Modelling of 3D microstructure and effective diffusivity of fly ash blended cement paste, Cem. Concr. Compos. 110 (2020), 103586.
[56] E. Sakai, S. Miyahara, S. Ohsawa, S.H. Lee, M. Daimon, Hydration of fly ash cement, Cem. Concr. Res. 35 (2005) 1135–1140.
[57] K. De Weerdt, M. Ben Haha, G. Le Saout, K.O. Kjellsen, H. Justnes, B. Lothenbach, Hydration mechanisms of ternary Portland cements containing limestone powder and fly ash, Cem. Concr. Res. 41 (2011) 279–291.
[58] G. Sant, C.F. Ferraris, J. Weiss, Rheological properties of cement pastes: A discussion of structure formation and mechanical property development, Cem. Concr. Res. 38 (2008) 1286–1296.
[59] W. Kunther, S. Ferreiro, J. Skibsted, Influence of the Ca/Si ratio on the compressive strength of cementitious calcium-silicate-hydrate binders, J. Mater. Chem. A. 5 (2017) 17401–17412.
[60] Y. Suda, T. Saeki, T. Saito, Y. Aono, F. Matsushita, S. Shibata, Y. Hama, T. Saeki, Relation between Chemical Composition and Physical Properties of C-S-H Generated from Cementitious Materials Nano-structural changes of C-S-H in Hardened Cement Paste during drying at 50°C Relation between Chemical Composition and Physical Properties of C-S-H Generated from Cementitious Materials, Go Igarashi J. Adv. Concr. Technol. 13 (2015) 275–290.
[61] N. Noguchi, S. Krishnya, T. Chabayashi, H. Kato, T. Nawa, Y. Elakneswaran, Hydration of ferrite-rich Portland cement: Evaluation of Fe-hydrates and Fe uptake in calcium-silicate-hydrates, Constr. Build. Mater. 288 (2021), 123142.
[62] L.P. Singh, A. Goel, S.K. Bhattacharyya, U. Sharma, G. Mishra, S.K. Bhattacharyy, S. Ahalawat, Hydration studies of cementitious material using silica nanoparticles Preparation of size controlled silica nano particles and its functional role in cementitious system Hydration Studies of Cementitious Material using Silica Nanoparticles, J. Adv. Concr. Technol. 13 (2015) 345–354.
[63] Z. Zhou, M. Sofi, E. Lumantarna, R. San Nicolas, G. Hadi Kusuma, P. Mendis, Strength Development and Thermogravimetric Investigation of High-Volume Fly Ash Binders, Materials (Basel) 12 (2019) 3344.
[64] E. Aydin, H.Ş. Arel, Characterization of high-volume fly-ash cement pastes for sustainable construction applications, Constr. Build. Mater. 157 (2017) 96–107.
[65] M. Rupasinghe, P. Mendis, T. Ngo, T.N. Nguyen, M. Sofi, Compressive strength prediction of nano-silica incorporated cement systems based on a multiscale approach, Mater. Des. 115 (2017) 379–392.
[66] K. Kinomura, T. Ishida, Enhanced hydration model of fly ash in blended cement and application of extensive modeling for continuous hydration to pozzolanic micro-pore structures, Cem. Concr. Compos. 114 (2020), 103733.
[67] P. Chindaprasirt, C. Jaturapitakkul, T. Sinsiri, Effect of fly ash fineness on compressive strength and pore size of blended cement paste, Cem. Concr. Compos. 27 (2005) 425–428.
[68] Y. Kocak, S. Nas, The effect of using fly ash on the strength and hydration characteristics of blended cements, Constr. Build. Mater. 73 (2014) 25–32.
[69] M. Hlobil, V. Šmilauer, G. Chanvillard, Micromechanical multiscale fracture model for compressive strength of blended cement pastes, Cem. Concr. Res. 83 (2016) 188–202.